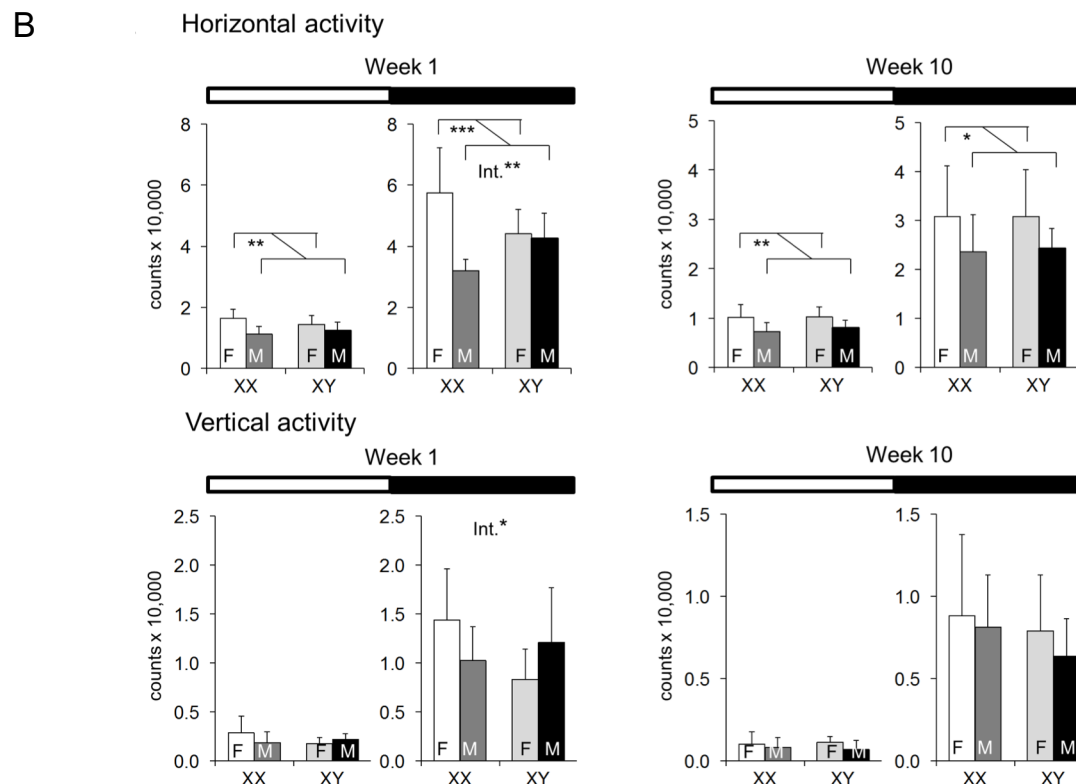
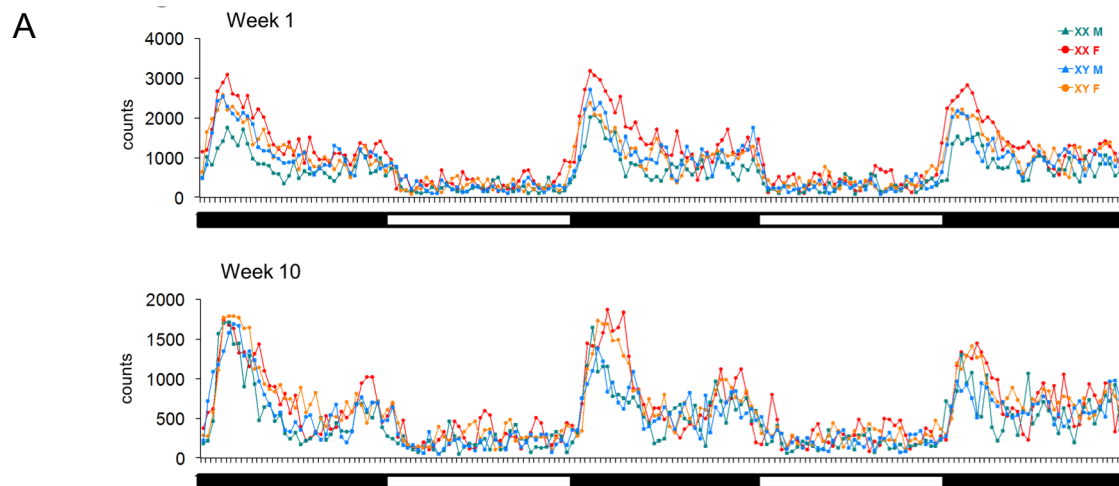


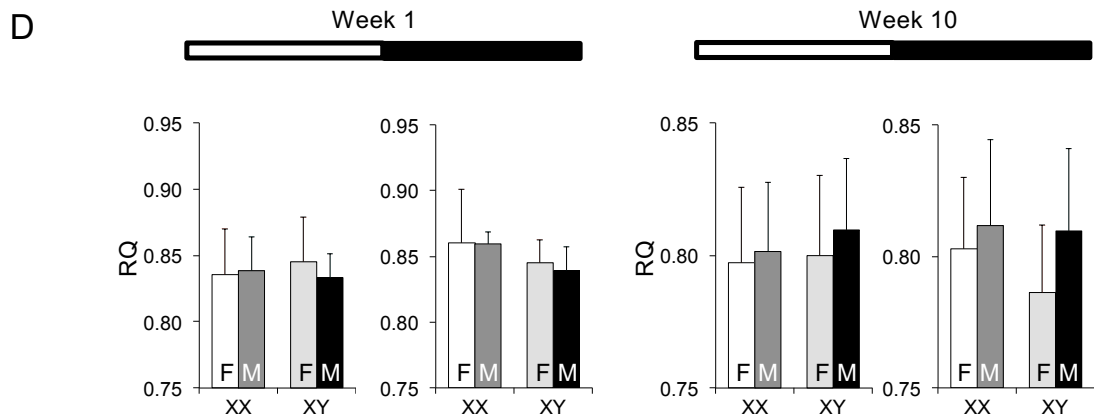
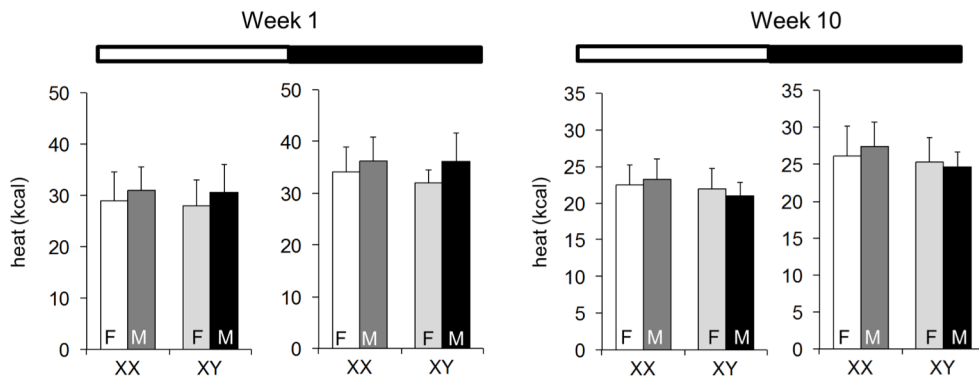
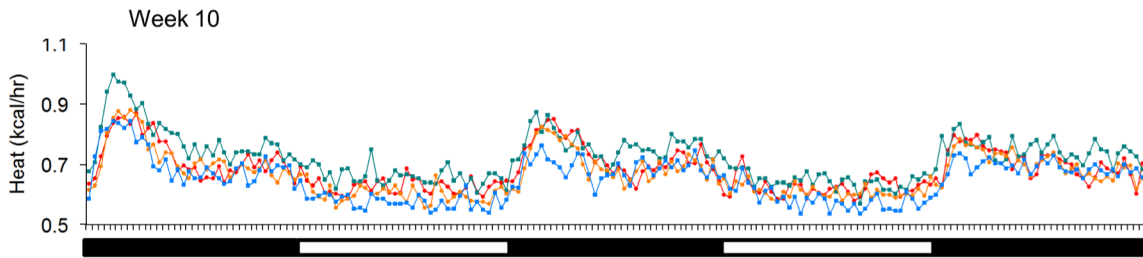
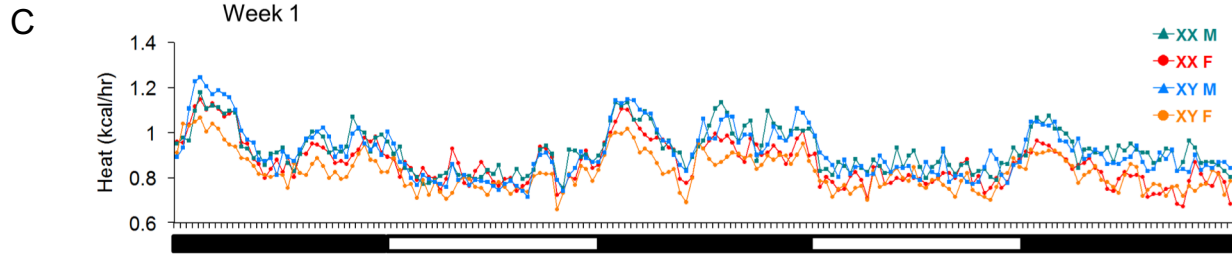
# Suppl. Fig. 1

## Physical activity and energy expenditure in FCG mice after 1 week and 10 weeks on high-fat diet.

(A) All four genotypes of FCG exhibited normal diurnal activity, with physical activity primarily during the dark phase of the circadian cycle. (B) Quantitation of horizontal and vertical activity. Female mice with ovaries showed higher horizontal locomotor activity than male mice. (C) Energy expenditure represented as heat generation, derived from Columbus Instruments Oxymax internal calculation of heat ( $[3.815 + 1.232 \times (\text{observed respiratory exchange ratio, RER})] \times (\text{observed oxygen consumption, } VO_2)$ ). We used this parameter rather than  $VO_2$  because it does not involve a body weight term, which can produce misleading results for groups of mice with different body weights, as occur between the genotypes in our study. (D) Respiratory quotient. Data were analyzed by 2-way ANOVA. Statistically significant differences are denoted by brackets. N = 4 mice per genotype. \*,  $p < 0.05$ ; \*\*,  $p < 0.01$ ; \*\*\*,  $p < 0.001$ . A significant interaction of sex chromosome complement and gonadal sex is denoted by "Int."



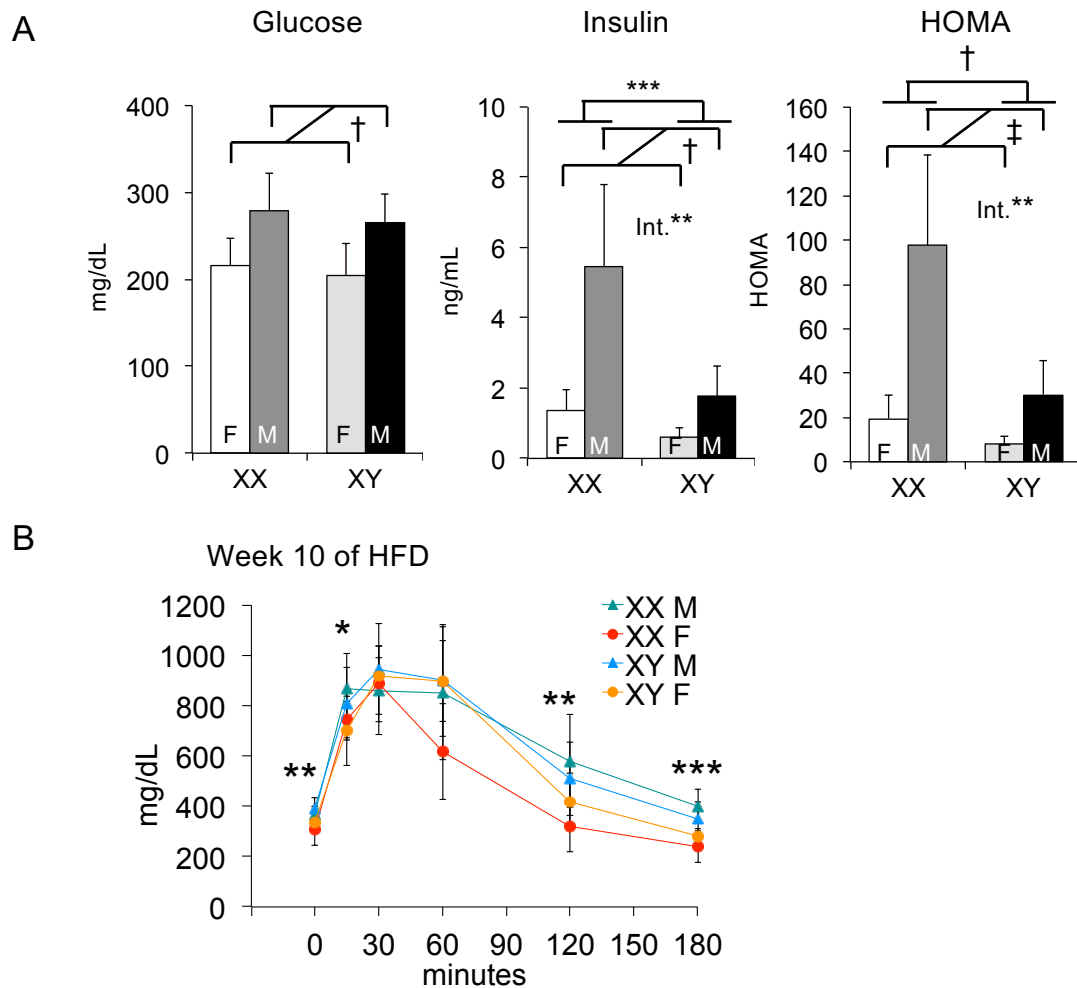
# Suppl. Fig. 1 (continued)



## Suppl. Fig. 2

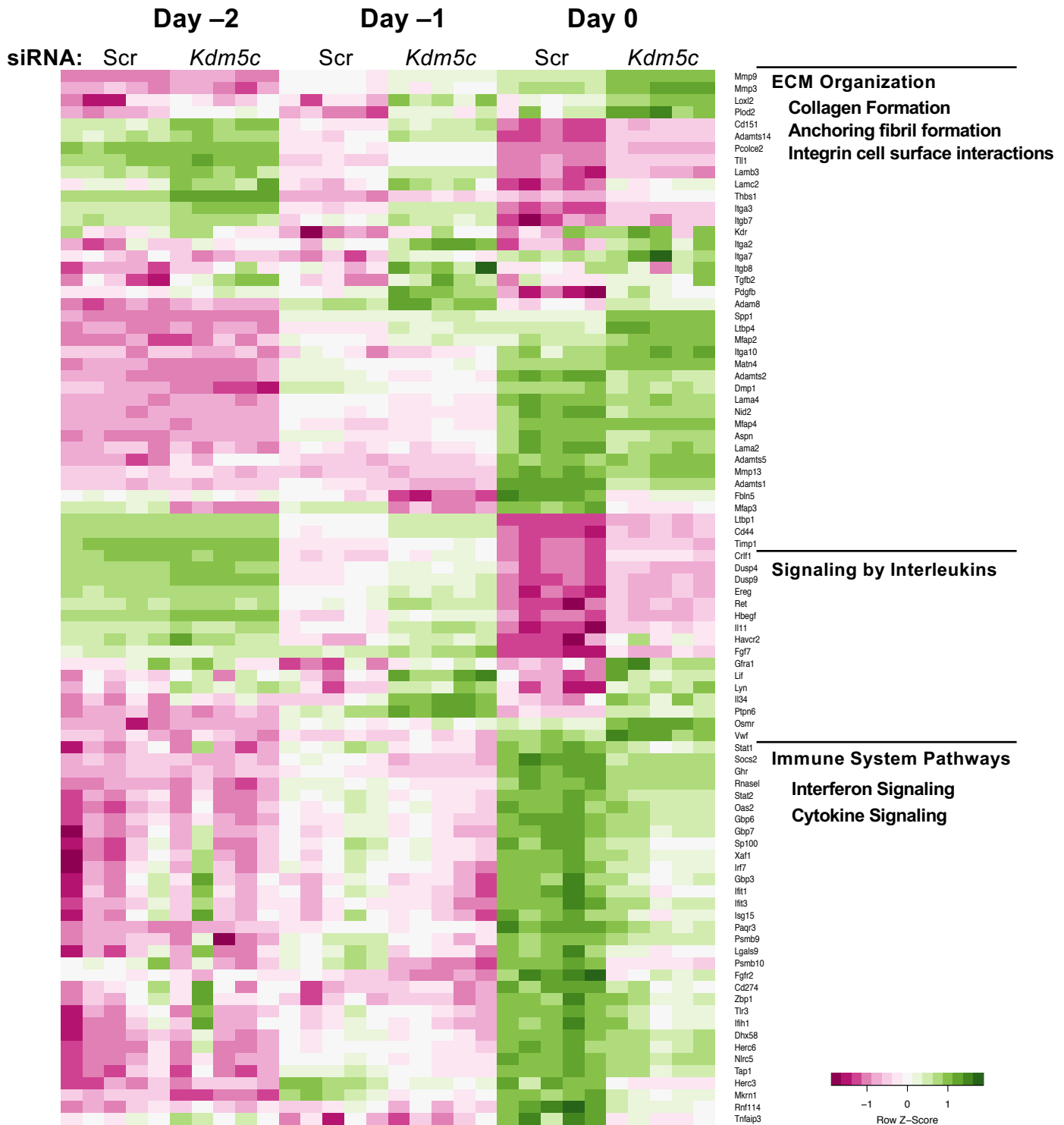
### Glucose and insulin FCG mice fed high-fat diet for 10 weeks.

(A) Fasting glucose, insulin and HOMA-IR for FCG mice fed high-fat diet for 10 weeks. Data were analyzed by 2-way ANOVA and statistically significant differences are denoted by brackets. (B) Glucose tolerance test following 10 months of high-fat diet. Data were analyzed by 2-way ANOVA and asterisks denote significant differences between males and females. There were no significant differences between XX and XY mice for glucose tolerance. N = 4–6 mice per genotype. \*,  $p < 0.05$ ; \*\*,  $p < 0.01$ ; \*\*\*,  $p < 0.001$ ; †,  $p < 0.0001$ ; ‡,  $p < 0.00001$ .



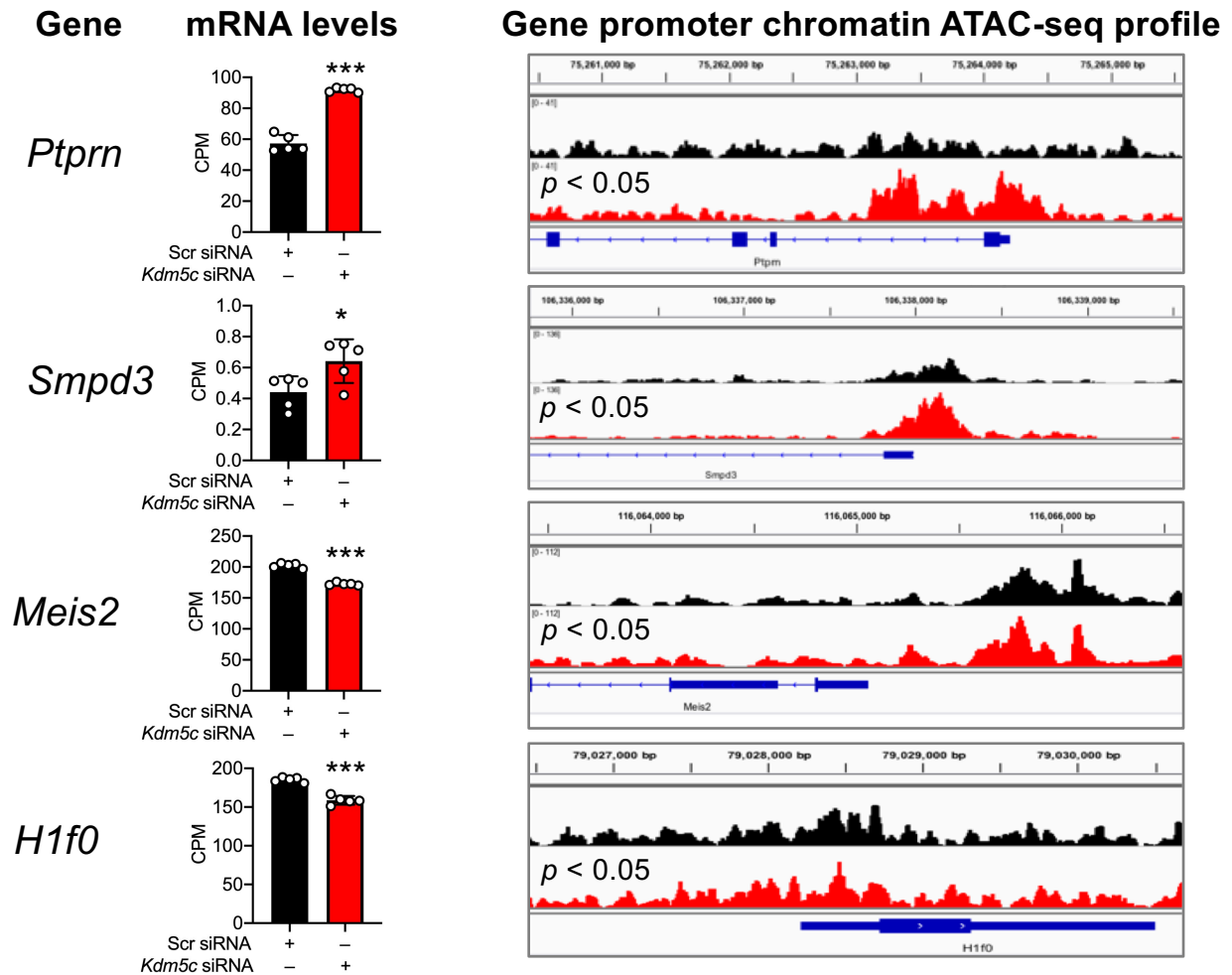
# Suppl. Fig. 3

Pathway enrichment for genes differentially expressed in 3T3-L1 cells treated with *Kdm5c* vs. control (Scr) siRNA. Heat map of differentially expressed genes in top pathways across all samples. N = 5 samples per treatment at each time point.



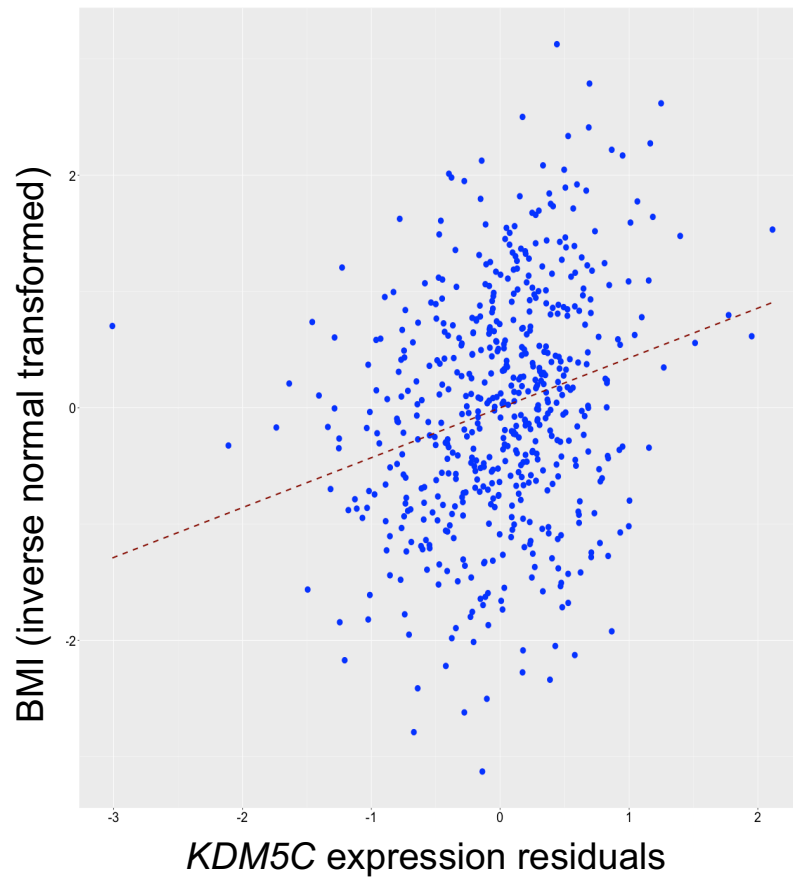
## Suppl. Fig. 4

Examples of correspondence between differential mRNA expression (RNA-seq) and ATAC-seq peaks. 3T3-L1 cells were treated with control of *Kdm5c* siRNA at Day -3 prior to confluence, and assessed at Day 0. N = 5 samples per treatment. **ATAC-seq peaks** are shown in red.



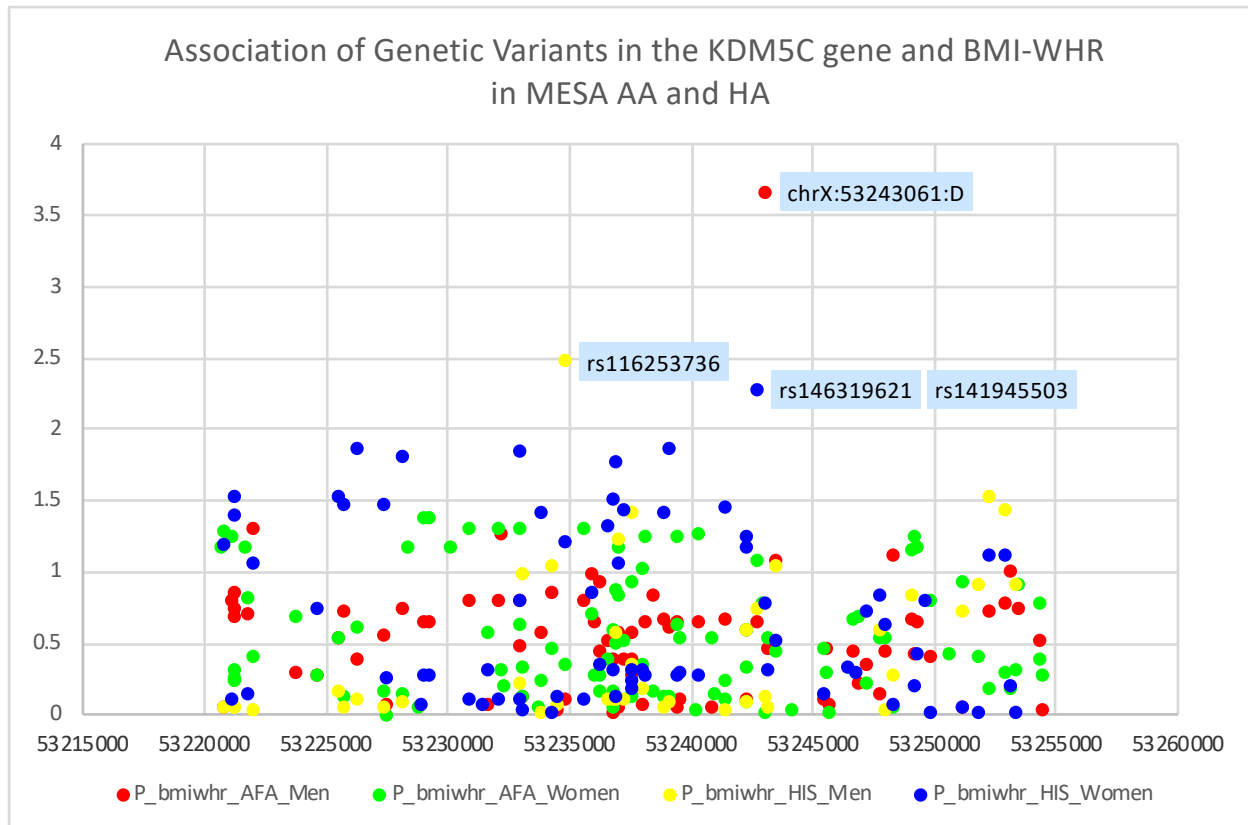
## Suppl. Fig. 5

**Correlation between *KDM5C* mRNA expression in human subcutaneous adipose tissue and body mass index (BMI).** Plot shows *KDM5C* expression residuals (x-axis) and inverse-normalized BMI (y-axis);  $p = 5 \times 10^{-10}$ . See main text and Methods sections for information on human subjects.



## Suppl. Fig. 6

***KDM5C* SNPs assessed for association with human BMI-WHR in the MESA African American and Hispanic American study samples.** X-axis denotes position along the human X chromosome; y-axis denotes  $-\log p$  for association. See main text and Methods sections for information on human subjects.



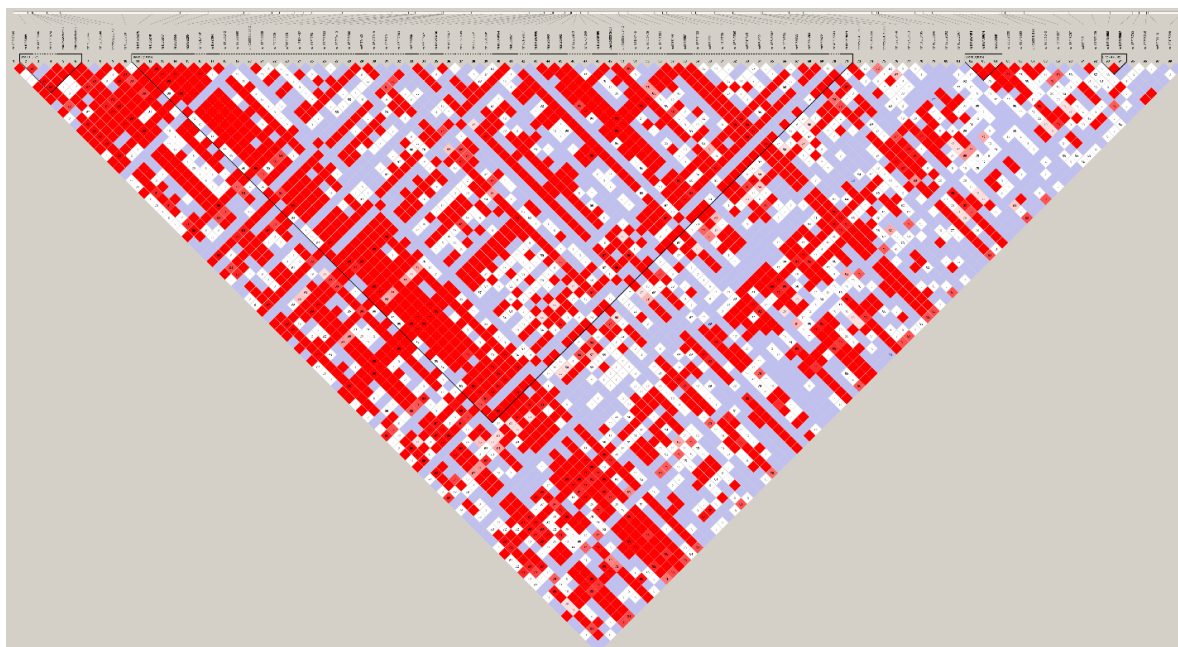
## Suppl. Fig. 7

Linkage disequilibrium (LD) structure of *KDM5C* gene in African American and Hispanic American individuals.

*KDM5C* LD structure in African American Men



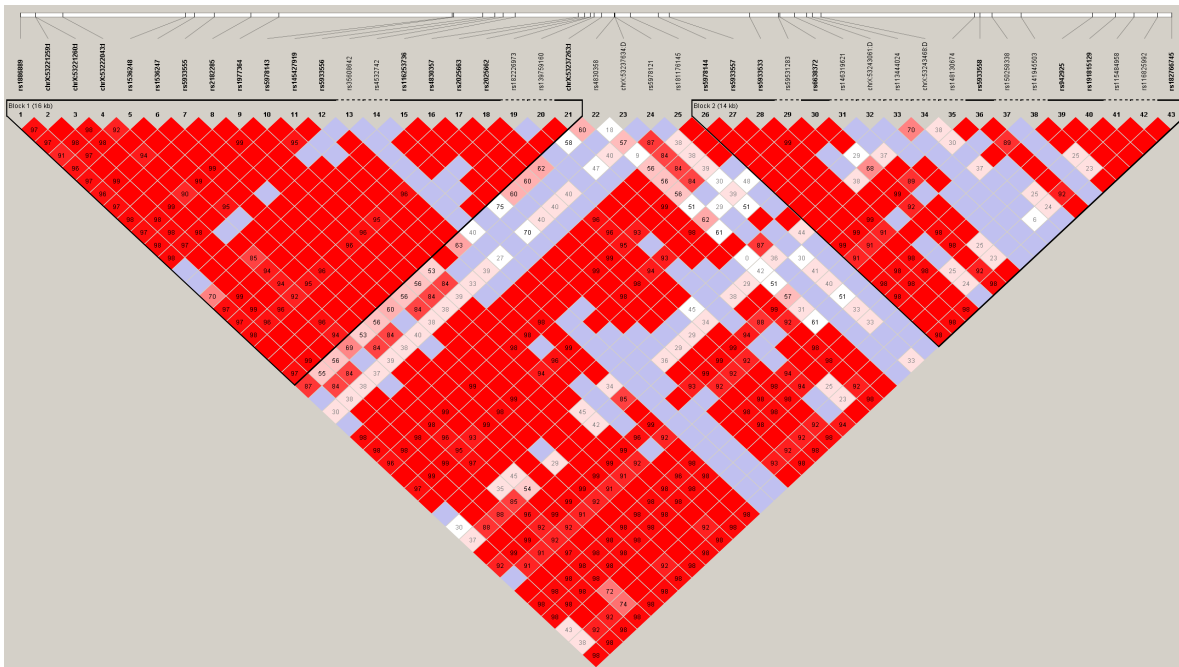
*KDM5C* LD structure in African American Women





# Suppl. Fig. 7 (continued)

## KDM5C LD structure in Hispanic American Men



## KDM5C LD structure in Hispanic American Women

